THE JOURNAL OF CHEMICAL PHYSICS **137**, 154707 (2012)

# Effect of spin-orbit coupling on the actinide dioxides $AnO_2$ (An=Th, Pa, U, Np, Pu, and Am): A screened hybrid density functional study

Xiao-Dong Wen,[1] Richard L. Martin,[1,a)] Lindsay E. Roy,[2] Gustavo E. Scuseria,[3] Sven P. Rudin,[1] Enrique R. Batista,[1] Thomas M. McCleskey,[4] Brian L. Scott,[4] Eve Bauer,[4] John J. Joyce,[5] and Tomasz Durakiewicz[5]

[1]*Theoretical Division, Los Alamos National Laboratory, Los Alamos, New Mexico 87545 USA*
[2]*Savanna River National Laboratory, Aiken, South Carolina 29808, USA*
[3]*Department of Chemistry, Department of Physics and Astronomy, Rice University, Houston, Texas 77251-1892, USA and Chemistry Department, Faculty of Science, King Abdulaziz University, Jeddah 21589, Saudi Arabia*
[4]*Materials Physics and Applications Division, Los Alamos National Laboratory, Los Alamos, New Mexico 87545, USA*
[5]*Condensed Matter and Thermal Physics Group, Los Alamos National Laboratory, Los Alamos, New Mexico 87545, USA*

(Received 4 July 2012; accepted 21 September 2012; published online 19 October 2012)

We present a systematic comparison of the lattice structures, electronic density of states, and band gaps of actinide dioxides, $AnO_2$ (An=Th, Pa, U, Np, Pu, and Am) predicted by the Heyd-Scuseria-Ernzerhof screened hybrid density functional (HSE) with the self-consistent inclusion of spin-orbit coupling (SOC). The computed HSE lattice constants and band gaps of $AnO_2$ are in consistently good agreement with the available experimental data across the series, and differ little from earlier HSE results without SOC. $ThO_2$ is a simple band insulator ($f^0$), while $PaO_2$, $UO_2$, and $NpO_2$ are predicted to be Mott insulators. The remainders ($PuO_2$ and $AmO_2$) show considerable O2*p*/An5*f* mixing and are classified as charge-transfer insulators. We also compare our results for $UO_2$, $NpO_2$, and $PuO_2$ with the PBE+U, self interaction correction (SIC), and dynamic mean-field theory (DMFT) many-body approximations. [http://dx.doi.org/10.1063/1.4757615]

## I. INTRODUCTION

The actinide oxides have been extensively studied in the context of the nuclear fuel cycle. They are also of fundamental interest as members of the class of strongly correlated materials – the Mott insulators – and a number of many-body approximations have been applied to their electronic structure.[1] We have previously reported the predictions of screened hybrid density functional theory across this series, and in particular have commented on the unexpected appearance of covalent mixing as one progress to the right in the series.[2] In the present contribution, we consider the effect of spin-orbit-coupling (SOC) on these results, and compare our results for the geometric structure, density of states (DOS), and band gaps with experiment and other theoretical approximations.

## II. COMPUTATIONAL DETAILS

The results in this paper are based on plane wave expansions using the computer program VASP (Vienna *Ab-initio* Simulation Package).[3] The energy cutoff for the plane-wave basis was set to 500 eV. Scalar relativistic effects are included with the PAW-PBE potentials[4,5] available in the distributed code. The Brillouin zone was sampled by Monkhorst-Pack meshes of 5 × 5 × 5 grid for hybrid density functional (HSE) calculations. This grid was tested at single points by expansion to 6 × 6 × 6. No significant differences were found. For the band structure calculations, 59 k-points were used. Convergence of the electronic degrees of freedom was met when the total energy change and the band structure energy change between two steps were both smaller than $1 \times 10^{-5}$. We relax all structural parameters (atomic position, lattice constants) using a conjugate-gradient algorithm until the Hellmann-Feynman forces are less than 0.01 eV/Å. Spin-orbit coupling has been implemented in VASP by Kresse and Lebacq.[6] The non-spherical contributions[7] from the gradient corrections inside the PAW spheres are considered in current calculations.

## III. RESULTS AND DISCUSSIONS

### A. Crystal structure of $AnO_2$

Figure 1 shows the well-known fcc $CaF_2$ fluorite structure, in which the actinide dioxides $AnO_2$ (An=Th, Pa, U, Np, Pu, and Am) appear with eight-coordinated An and four-coordinated O. If one takes oxygen as divalent, the stoichiometry implies $An^{4+}$ and $2O^{2-}$. $UO_2$ is known to order antiferromagnetically, assuming the AFM-I spin motif as marked in Figure 1 by black arrows. The other members of the series have more complex magnetic ordering motifs that are beyond the scope of the present work. We focus here on the properties of the ferromagnetic (FM) and AFM-I states.

a)Author to whom correspondence should be addressed. Electronic mail: rlmartin@lanl.gov.

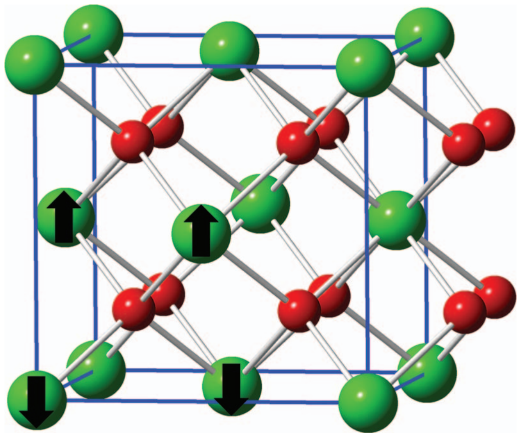

FIG. 1. The fluorite crystal structure exhibited by $AnO_2$, where An=Th, Pa, U, Np, Pu, and Am. O atoms = red balls, An atoms = green balls. The black arrows illustrate the (100) AFM ordering.

### B. Calculated parameters of $AnO_2$ (An=Th, Pa, U, Np, Pu, and Am)

Table I reports the relative energies, lattice constants, magnetic moments (AFM), and band gaps (AFM) for AFM and FM states of the $AnO_2$ series with HSE and HSE+SOC. One can see that there are no large changes in the properties associated with inclusion of SOC. The HSE generally predicts AFM ordered $AnO_2$ to be more favorable than the corresponding FM states.

The SOC generally decreases the splitting between AFM and ferromagnetic states. In $PaO_2$, $PuO_2$, and $AmO_2$ this leads to very small Heisenberg couplings – of the order of 10–50 meV. The lone exception is $NpO_2$, where inclusion of SOC changes the predicted ground state from ferromagnetic to AFM-I. The calculated band gaps and lattice constants (from HSE and HSE+SOC) are in good agreement with the corresponding experimental values, as shown in Table I and Figure 2. We note that the band gaps in Table I were extracted from a numerical tabulation of the gap vs. k point. These values are slightly different from those inferred from the DOS plots. We were advised by the VASP team that the direct examination of the numerical data is preferred.

The values for the unpaired spin density on the metal site follow that expected from the formal valences very closely, and are affected very little by SOC (see supplementary material[33]). The calculated magnetic moment for U (1.95 $\mu_B$) in the dioxide agrees well with the experimental value of 1.8–2.0 $\mu_B$[8] (see Table I). However, the corresponding magnetic moments on the metal in $NpO_2$ and $PuO_2$ of 2.92 and 3.91 $\mu_B$, respectively, differ significantly from their corresponding experimental observation, 0.4 $\mu_B$[9] or something similarly small[10,11] for Np and no moment for Pu.[12] The discrepancy in the former likely stems from the complex magnetic ordering issues, and the absence of a moment in the latter from atomic multiplet effects difficult to address within density functional theory (DFT). The magnetic ground states involve a competition between states differing very little in energy, and remain a significant challenge for theory.

There is an additional point worth making here. We sometimes see significant differences in the computed band gaps depending on whether we are studying the antiferromagnetic or ferromagnetic phase. For example, the band gap for $UO_2$ in the AFM phase is ~2.4 eV, while it becomes 2.2 eV in the ferromagnetic phase. The experimental result is 2.1 eV. Most of the measurements of the optical gap are made above the Néel temperature, and so it is not clear which of our theoretical values should be compared with experiment. The closed-shell, nonmagnetic, electronic state lies much higher in energy than the Néel temperature, and is surely not the appropriate state with which to compare. Presumably, the experimental paramagnet is most similar to the underlying AFM

TABLE I. Calculated relative energies for AFM and FM $AnO_2$ (An=Th, Pa, U, Np, Pu, and Am) from HSE and HSE+SOC, respectively, as well the calculated AFM gap and magnetic moment.

| | | $E_{rel.}$ (eV) | | $a_0$ (Å) | | $\mu(\mu_B)$ | Gap (eV) VASP | Gap (eV) Gaussian[2] |
|---|---|---|---|---|---|---|---|---|
| | | AFM | FM | AFM | FM | AFM | AFM | AFM |
| $ThO_2$ | HSE | 0.00 | 0.00 | 5.586 | 5.586 | 0.00 | 6.0 | 6.1 |
| | HSE+SOC | 0.00 | 0.00 | 5.580 | 5.580 | 0.00 | 5.8 | 6.1 |
| | Expt. | | | 5.602 (Ref. 13) | | 0.00 | 5.75 (Ref. 13) | |
| $PaO_2$ | HSE | 0.00 | 0.25 | 5.501 | 5.483 | 0.94 | 1.2 | 1.1 |
| | HSE+SOC | 0.00 | 0.02 | 5.499 | 5.494 | 0.95 | 1.5 | 1.2 |
| | Expt. | | | 5.505 (Ref. 14) | | ... | ... | |
| $UO_2$ | HSE | 0.00 | 0.19 | 5.458 | 5.418 | 1.98 | 2.4 | 2.8 |
| | HSE+SOC | 0.00 | 0.10 | 5.457 | 5.457 | 1.95 | 2.4 | 2.7 |
| | Expt. | | | 5.470 (Ref. 15) | | 1.8 ~ 2.0 (Ref. 8) | 2.10 (Ref. 16) | |
| $NpO_2$ | HSE | 0.00 | −0.12 | 5.412 | 5.411 | 3.00 | 2.4 | 3.0 |
| | HSE+SOC | 0.00 | 0.15 | 5.418 | 5.418 | 2.92 | 2.4 | 3.0 |
| | Expt. | | | 5.434 (Ref. 17) | | ~0.4 | 2.85 (Ref. 18) | |
| $PuO_2$ | HSE | 0.00 | 0.15 | 5.383 | 5.378 | 4.00 | 2.4 | 2.6 |
| | HSE+SOC | 0.00 | 0.01 | 5.379 | 5.373 | 3.91 | 2.6 | 2.6 |
| | Expt. | | | 5.398 (Ref. 19) | | 0.00 (Ref. 12) | 2.80 (Ref. 18) | |
| $AmO_2$ | HSE | 0.00 | 0.23 | 5.375 | 5.362 | 4.99 | 1.5 | 1.5 |
| | HSE+SOC | 0.00 | 0.05 | 5.357 | 5.355 | 4.96 | 1.5 | 1.5 |
| | Expt. | | | 5.376 (Ref. 20) | | ... | 1.30 (Ref. 21) | |

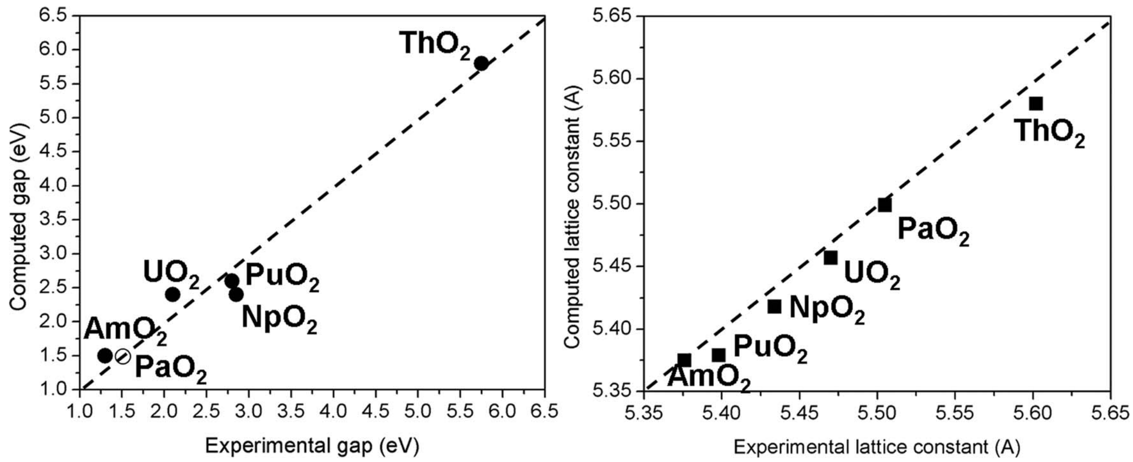


FIG. 2. Left: The computed gap (HSE) versus the experimental gap of $AnO_2$ (An=Th, Pa, U, Np, Pu, and Am). The dashed line has a slope of unity. Note the circle for $PaO_2$ represents only a computed value, as we are not aware of an experimental result. Right: The computed lattice constant (HSE) versus the experimental lattice parameter for the $AnO_2$ series.

result with disordered moments, and so that is what we have reported here. In principle, we should do a calculation on a unit cell large enough to simulate the disordered paramagnetic phase, but that is presently beyond our capabilities. Finally, we note that the band gaps quoted in Table I for $NpO_2$ and $PuO_2$, 2.85 eV and 2.8 eV[18] differ significantly from those in the earlier literature, 0.4 eV[22] for $NpO_2$ and 1.8 eV[23] for $PuO_2$. The previous literature values were inferred from optical conductivity measurements, whereas the more recent measurements utilized direct optical absorption on single crystal quality thin films. The band gaps from our calculations, even those published earlier which did not include SOC, are in good agreement with these new measurements.

The values in Figure 2 were obtained from VASP with a plane-wave basis set, the PAW treatment of the relativistic core, and a spin-orbit correction. We have also computed these properties with the *Gaussian* suite of electronic structure codes using a basis set of Gaussian orbitals and the relativistic effective core potentials described previously,[2] in conjunction with the SOC methodology described by Peralta *et al.*[24] It is gratifying that the results agree fairly well between the two approaches (Table I). The largest discrepancy occurs for $NpO_2$, where the gaps differ by some 0.6 eV. The origin of this discrepancy is unknown, but may arise from the differing basis sets, representations of the relativistic core, and manner in which the spin-orbit coupling is approximated. We are investigating these issues now.

### C. Calculated density of states of $AnO_2$ from HSE and HSE+SOC

The DOS of the AFM-I phase of $AnO_2$ from HSE+SOC shown in Figure 3 are similar to those from HSE (see supplementary material). We can see that among these oxides, $PaO_2$, $UO_2$, and $NpO_2$ are Mott insulators, with the gap associated with an An5*f* to An5*f* transition. At $PuO_2$ the 5*f* band becomes nearly degenerate with the O2*p* band, which is reflected in the distinctly mixed An5*f*-O2*p* character of the valence band as shown in the partial DOS in Figure 3. The conduction band remains nearly pure An5*f*, and so we associate $PuO_2$ through $AmO_2$ as ligand-to-metal charge-transfer (LMCT) insulators (O2*p* to An5*f*). These classifications are in agreement with the earlier work in a localized basis set.[2] The appearance of significant An5*f*/O2*p* mixing arises from the increasing stabilization of the An 5*f* band due to incomplete shielding of the nuclear charge as one proceeds across the actinide series. The An5*f* band becomes nearly degenerate with the O2*p* band in the region of Pu, and results in a near degeneracy mixing (see Scheme 1), as commented on previously.[2,25] In our previous work,[2] the spin density on the metal was observed to increase incrementally in early members of the An series in just the way expected from formal f-orbital occupations based upon $An^{4+}$ ions; at Cm, however, evidence of an intermediate valence ($Cm^{3+}$/$Cm^{4+}$) emerged. This is also true of the present results with spin-orbit coupling. A discussion of the results for $CmO_2$ is deferred to a subsequent paper. Additional information (on the spin density and integrations of f states) for all the actinide dioxides is given in the supplementary material.

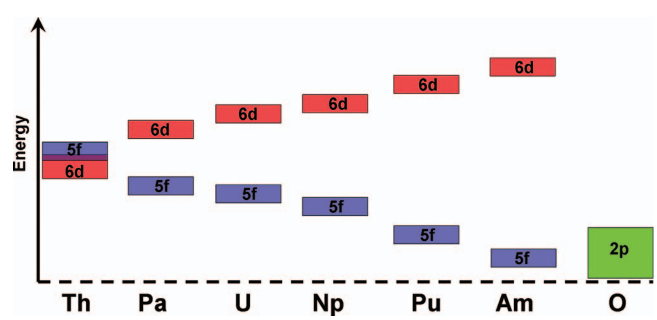


SCHEME 1. Schematic of the atomic orbital energy levels for Th, Pa, U, Np, Pu, Am, and the O2*p* band. The 5*f* orbital energy decreases steadily across the row, becoming nearly degenerate with the O2*p* band beginning with Pu. This leads to a metal-ligand mixing proportional to a Hamiltonian matrix element between the An5*f* and the O2*p* orbitals divided by the orbital energy difference. Although the matrix element decreases steadily across the row as the actinide 5*f* orbital contracts, it is offset by the energy denominator which becomes small for the later member of the row, leading to significant mixing and predictions of covalency in the calculations.

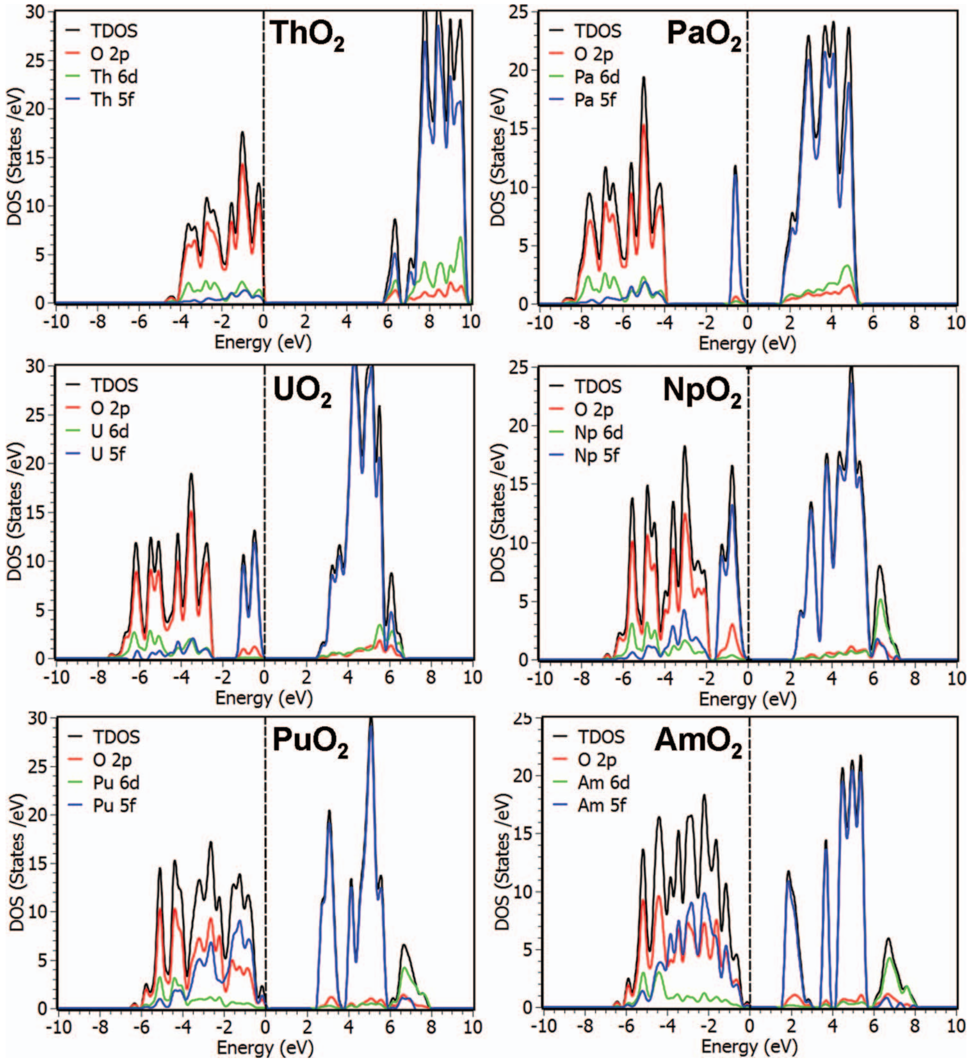


FIG. 3. The calculated density of states of AFM $AnO_2$ (An=Th, Pa, U, Np, Pu, and Am) from the HSE approximation with spin-orbital coupling. The magnitudes of the gap in these figures are slightly from those in Table II.

### D. Comparing the lattice constants and band gaps to other approximations

Other approximations have been applied to these actinide materials, including a number of DFT+U studies.[26] They are generally capable of giving a reasonable band gap, given a judicious choice for the empirical parameter U, but we have found that the U which reproduces the band gap often yields significant errors in other metrics such as the lattice constant. We have performed PBE+U calculations on the series, with a $U_{eff.}$ (=U − J) for all actinides set to 4 eV. As shown in Table II, the lattice constants of $UO_2$, $NpO_2$, and $PuO_2$ calculated by PBE+U are much longer than the corresponding experimental value. PBE+U predicts $ThO_2$ as a charge-transfer insulator with a band gap of 4.7 eV, smaller than the experimental gap by 1 eV, while the insulating oxides $PaO_2$ and $AmO_2$ are predicted to be metallic.

Most recently Yin *et al.*[27] have applied dynamic mean-field theory (DMFT) to $UO_2$, $NpO_2$, and $PuO_2$. In contrast to their earlier DMFT work[28] in which the most important parameter in the theory, the on-site repulsion U, was determined empirically, they have now determined U "*ab initio*". The consequence of this is that while the early work described $UO_2$ as a Mott insulator, the most recent work finds it to be a charge-transfer insulator, and the ground state to be Zhang-Rice singlet in nature. This conclusion is in contradiction with photoemission results, which show 5*f* character at the Fermi energy, as well as a recent comprehensive x-ray absorption study by Yu *et al.*[29,30] and femtosecond pump-probe studies[31] which firmly establish $UO_2$ as a Mott-Hubbard insulator. Femtosecond pump-probe studies have also followed ultrafast hopping dynamics of 5*f* electrons in $UO_2$. The major difference between the two studies is the much larger value for U (6 eV)[27] determined "*ab initio*" versus the earlier empirical value of 3 eV.[28] The result is similar to what is seen in LDA+U studies where a value for U that is too large pushes the *f* states too far down into the O2*p* based levels. This is likely the cause of the problem here.

Petit *et al.*[32] have studied actinide monoxides, sesquioxides and dioxides (An = U...Cf) using the silicon integrated circuit (SIC) approximation. The dioxides, with the exception of $UO_2$, are generally found to be insulating. Interestingly, the most stable configuration for $UO_2$ is found to be a

TABLE II. Comparison of various approximations for the lattice constant (Å), band gap (eV), and insulator classification for $AnO_2$ (An=Th, Pa, U, Np, Pu, and Am), as well as experiment.

| | | Band gap (eV) | Latt. Const. (Å) | Classification |
|---|---|---|---|---|
| $ThO_2$ | HSE (VASP)[a] | 5.8 | 5.580 | Charge-transfer |
| | HSE (Gaussian) (Ref. 2) | 6.2 | 5.595 | Charge-transfer |
| | PBE+U[a] | 4.7 | 5.671 | Charge-transfer |
| | Expt. | 5.75 (Ref. 13) | 5.602 (Ref. 13) | ... |
| $PaO_2$ | HSE (VASP)[a] | 1.5 | 5.499 | Mott-Hubbard |
| | HSE (Gaussian) (Ref. 2) | 1.4 | 5.518 | Mott-Hubbard |
| | PBE+U[a] | 0.0 | 5.544 | ... |
| | Expt. | ... | 5.505 (Ref. 14) | ... |
| $UO_2$ | HSE (VASP)[a] | 2.4 | 5.458 | Mott-Hubbard |
| | HSE (Gaussian) (Ref. 2) | 2.6 | 5.463 | Mott-Hubbard |
| | PBE+U[a] | 2.3 | 5.568 | Mott-Hubbard |
| | SIC (Ref. 32) | 0.0[b] | 5.400 | ... |
| | DMFT (Ref. 27) | 2.5 | ... | Charge-transfer |
| | Expt. | 2.1 (Ref. 16) | 5.470 (Ref. 15) | Mott-Hubbard (Refs. 29–31) |
| $NpO_2$ | HSE (VASP)[a] | 2.4 | 5.412 | Mott-Hubbard |
| | HSE (Gaussian) (Ref. 2) | 2.8 | 5.430 | Mott-Hubbard |
| | PBE+U[a] | 2.6 | 5.498 | Charge-transfer |
| | SIC (Ref. 32) | 2.3 | 5.460 | Charge-transfer |
| | DMFT (Ref. 27) | ... | ... | ... |
| | Expt. | 2.85 (Ref. 18) | 5.434 (Ref. 17) | ... |
| $PuO_2$ | HSE (VASP)[a] | 2.6 | 5.383 | Charge-transfer |
| | HSE (Gaussian) (Ref. 2) | 2.8 | 5.396 | Charge-transfer |
| | PBE+U[a] | 1.6 | 5.465 | Charge-transfer |
| | SIC (Ref. 32) | 1.2 | 5.440 | Charge-transfer |
| | DMFT (Ref. 27) | ~3.5 | ... | Charge-transfer |
| | Expt. | 2.80 (Ref. 18) | 5.398 (Ref. 19) | ... |
| $AmO_2$ | HSE (VASP)[a] | 1.5 | 5.357 | Charge-transfer |
| | HSE (Gaussian) (Ref. 2) | 1.6 | 5.369 | Charge-transfer |
| | PBE+U[a] | 0.0 | 5.425 | ... |
| | SIC (Ref. 32) | 0.8 | 5.420 | Charge-transfer |
| | Expt. | 1.3 (Ref. 21) | 5.376 (Ref. 20) | |

[a]Current work; $U_{eff}$ = 4.0 eV in PBE+U calcultions.
[b]The SIC finds an insulating state with a gap of 2.6 eV (a charge-transfer insulator), only 100 meV higher than this metallic ground state.

U(V), $f^1$, species, which is metallic. They point out that the U(IV), $f^2$, state lies only 100 meV higher in energy, and it is gapped by 2.6 eV, in good agreement with the HSE results. The gap, however, is charge transfer in nature, as was the case for the DMFT results. The ground states of $NpO_2$ and $PuO_2$ are found to be tetravalent with the SIC. It is interesting that the An5*f*/O2*p* orbital mixing with SIC decreases with increasing Z; an intuitively appealing result, but in contrast to the hybrid DFT predictions.

For completeness, the dielectric functions and optical spectrum of $UO_2$, $NpO_2$, and $PuO_2$ predicted by HSE and PBE+U approaches are given in the supplementary material.

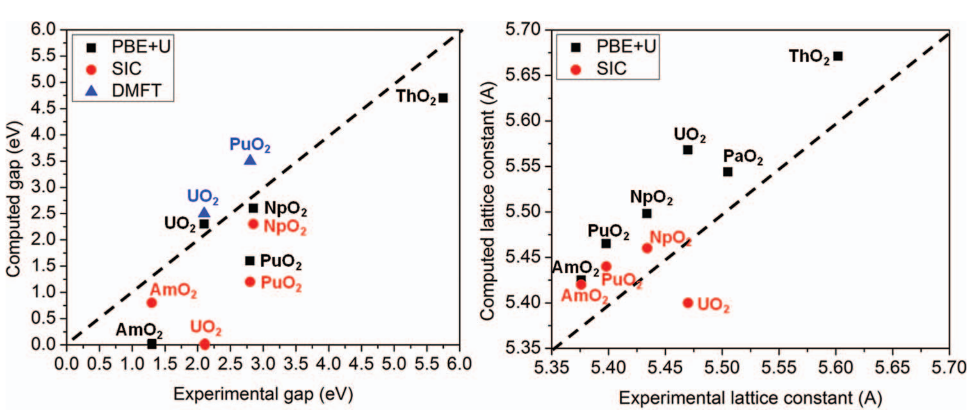


FIG. 4. Left: Correlation of experimental gap for $AnO_2$ with computed gap from various approximations. Right: Correlation of experimental lattice constant with computed lattice constant from various approximations. We were unable to find lattice constants reported with DMFT.

In general, both approaches are in qualitative agreement with experiment.

## IV. CONCLUSIONS

We conclude that the HSE functional gives a reasonably faithful reproduction of the band gaps and lattice constants for these actinide dioxides when compared with available experimental data (Figure 2). A similar plot of lattice constants and band gaps of various approximations with experiment is given in Figure 4. With a judicious choice of the parameter U, the DFT+U approximations appear to be capable of yielding reasonable band gaps. This occurs at the expense of other important properties such as the lattice constant and the density of states. In addition to the magnitude of the band gap, these approximations differ in their assignments of the origin. HSE and PBE+U correctly describe $UO_2$ as a Mott insulator, while the SIC and the most recent DMFT approximations incorrectly predict the early members of this series to be charge-transfer insulators.

In conclusion, HSE performs quite well for this series of Mott insulators. It is particularly encouraging that unlike the DFT+U and practical implementations of DMFT, *it does not require the introduction of material specific parameters*. Problems remaining to be addressed include multiplet effects, and the proper treatment of the complex magnetic properties of these oxides.

## ACKNOWLEDGMENTS

The work at Los Alamos National Laboratory was supported under the Heavy Element Chemistry Program at LANL by the Division of Chemical Sciences, Geosciences, and Biosciences, Office of Basic Energy Sciences, U.S. Department of Energy. Los Alamos National Laboratory is operated by Los Alamos National Security, LLC, for the National Nuclear Security Administration of U.S. Department of Energy under contract DE-AC52-06NA25396 and the LDRD program at LANL. X.-D. Wen gratefully acknowledges a Seaborg Institute Fellowship. The work at Rice University is supported by DOE, Office of Basic Energy Sciences, Heavy Element Chemistry program under Grant No. DE-FG02-04ER15523. Some of the calculations were performed on the Chinook computing systems at the Molecular Science Computing Facility in the William R. Wiley Environmental Molecular Sciences Laboratory (EMSL) at PNNL. The Los Alamos National Laboratory is operated by Los Alamos National Security, LLC, for the National Nuclear Security Administration of the U.S. Department of Energy under Contract No. DE-AC5206NA25396.

[1] N. F. Mott, Proc. Phys. Soc., London, Sect. A **62**, 416 (1949).
[2] I. D. Prodan, G. E. Scuseria, and R. L. Martin, Phys. Rev. B **76**, 033101 (2007).
[3] G. Kresse and J. Hafner, Phys. Rev. B **47**, 558 (1993).
[4] P. E. Bloechl, Phys. Rev. B **50**, 17953 (1994).
[5] G. Kresse and D. Joubert, Phys. Rev. B **59**, 1758 (1999).
[6] G. Kresse and O. Lebacq, VASP manual, see http://cms.mpi.univie.ac.at/vasp/.
[7] See VASP online manual at http://cms.mpi.univie.ac.at/vasp/vasp/LASPH_tag.html.
[8] *Los Alamos Science*, edited by N. G. Cooper (Los Alamos National Laboratory, Los Alamos, NM, 2000), Vol. 26.
[9] P. Eedös, G. Solt, A. Żolnierek, A. Blaise, and J. M. Fournier, Physica B + C **102**, 164 (1980).
[10] D. Mannix, G. H. Lander, J. Rebizant, R. Caciuffo, N. Bernhoeft, E. Lidström, and C. Vettier, Phys. Rev. B **60**, 15187 (1999).
[11] R. Caciuffo, J. A. Paixão, C. Detlefs, M. J. Longfield, P. Santini, N. Bernhoeft, J. Rebizant, and G. H. Lander, J. Phys.: Condens. Matter **15**, S2287 (2003).
[12] H. Yasuoka, G. Koutroulakis, H. Chudo, S. Richmond, D. K. Veirs, A. I. Smith, E. D. Bauer, J. D. Thompson, G. D. Jarvinen, and D. L. Clark, Science **336**, 901 (2012).
[13] O. D. Jayakumara, I. K. Gopalakrishnana, A. Vinub, A. Asthanac, and A. K. Tyagia, J. Alloys Compd **461**, 608 (2008).
[14] P. A. Sellers, S. Fried, E. Elson, and W. H. Zachariasen, J. Am. Chem. Soc. **76**, 5935 (1954).
[15] J. Schoenes, J. Appl. Phys. **49**, 1463 (1978).
[16] S. Kern, R. A. Robinson, H. Nakotte, G. H. Lander, B. Cort, P. Wason, and F. A. Vigil, Phys. Rev. B **59**, 104 (1999).
[17] T. Yamashita, N. Nitani, T. Tsuji, and H. Inagaki, J. Nucl. Mater. **247**, 90 (1997).
[18] T. M. McCleskey, E. Bauer, Q. Jia, A. K. Burrell, B. L. Scott, S. D. Conradson, A. Mueller, L. E. Roy, X.-D. Wen, G. E. Scuseria, and R. L. Martin, "Optical band gap of $NpO_2$ and $PuO_2$ from optical absorbance of epitaxial films," J. Appl. Phys. (in press).
[19] J. M. Haschke, T. H. Allen, and L. A. Morales, Science **287**, 285 (2000).
[20] L. B. Asprey, F. H. Ellinger, S. Fried, and W. H. Zachariasen, J. Am. Chem. Soc. **77**, 1707 (1955).
[21] C. Suzukia, T. Nishia, M. Nakadaa, M. Akaboria, M. Hiratab, and Y. Kajia, J. Phys. Chem. Solids **73**, 209 (2012).
[22] J. M. Fournier and R. Troć, in *Handbook on the Physics and Chemistry of the Actinides*, edited by A. J. Freeman and G. H. Lander (North Holland, Amsterdam, 1985), Vol. 2, Chap. 2.
[23] C. E. McNeilly, J. Nucl. Mater. **11**, 53 (1964).
[24] J. E. Peralta, J. Heyd, G. E. Scuseria, and R. L. Martin, Phys. Rev. B **74**, 073101 (2006).
[25] M. L. Neidig, D. L. Clark, and R. L. Martin, Coord. Chem. Rev., available at http://dx.doi.org/10.1016/j.ccr.2012.04.029.
[26] A. Modin, Y. Yun, M.-T. Suzuki, J. Vegelius, L. Werme, J. Nordgren, P. M. Oppeneer, and S. M. Butorin, Phys. Rev. B **83**, 075113 (2011).
[27] Q. Yin, A. Kutepov, K Haule, G. Kotliar, S. Y. Savrasov, and W. E. Pickett, Phys. Rev. B **84**, 195111 (2011).
[28] Q. Yin and S. Y. Savrasov, Phys. Rev. Lett. **100**, 225504 (2008).
[29] S.-W. Yu, J. G. Tobin, J. C. Crowhurst, S. Sharma, J. K. Dewhurst, P. O. Velasco, W. L. Yang, and W. J. Siekhaus, Phys. Rev. B **83**, 165102 (2011).
[30] J. G. Tobin and S.-W. Yu, Phys. Rev. Lett. **107**, 167406 (2011).
[31] Y. An, A. J. Taylor, S. D. Conradson, S. A. Trugman, T. Durakiewicz, and G. Rodriguez, Phys. Rev. Lett. **106**, 207402 (2011).
[32] L. Petit, A. Svane, Z. Szotek, W. M. Temmerman, and G. M. Stocks, Phys. Rev. B **81**, 045108 (2010) and references therein.
[33] See supplementary material at http://dx.doi.org/10.1063/1.4757615 for (1) Calculated density of states from HSE; (2) Calculated band structure of $AnO_2$ (An=Th, Pa, U, Np, Pu and Am) from HSE+SOC; (3) Spin density and integrations of f states for $AnO_2$ (An=Th, Pa, U, Np, Pu, Am); (4) TDOS of FM $NpO_2$ by HSE and PBE+U; and (5) Calculated dielectric function and optical spectrum of $UO_2$, $NpO_2$, and $PuO_2$.